Mathematical Modeling and Optimization of the Dehydrogenation of Ethylbenzene to Form Styrene

A mathematical model is developed for a styrene pilot plant reactor. The steady state version of this model was used to optimize the location of a steam injection port part way along the catalytic bed. Significant improvement in reactor performance was predicted by splitting the steam feed between the reactor inlet and the injection port. Performance was measured in terms of market value of products minus a utility cost for the steam. Studies were also carried out via computer simulation to determine optimal operating conditions. An important result was the relationship of optimal steam-to-ethylbenzene feed ratio to the kinetic parameters which describe the main dehydrogenation reaction. A pilot plant was constructed and operated in order to investigate experimentally the predictions of the mathematical model. Instrumentation was designed and installed so that an on-line digital computer could acquire process measurements directly and establish operating conditions. The experimental program confirmed the improved performance by operation of the reactor with a steam injection port and the existence of an optimum of the steam-to-ethylbenzene feed ratio as indicated by simulation.

DAVID E. CLOUGH
and
W. FRED RAMIREZ
Department of Chemical Engineering
University of Colorado
Boulder, Colorado 80302

SCOPE

The development of industrial chemical processes and their operation have for the most part been carried out by empirical methods. The approach used here employs modern techniques of mathematical modeling, computer simulation, and optimization. Catalytic dehydrogenation of ethylbenzene to produce styrene monomer is the process considered. A mathematical model is derived based on fundamental principles of chemical kinetics and transport phenomena. This model is then simplified using scaling arguments. The mathematical model is used via computer simulation to choose an important design parameter, the optimal location along the tubular reactor of a steam injection port, and also to investigate the most profitable operating conditions and their dependence on reaction parameters.

A pilot plant was designed and constructed, and one of the tubular reactors tested was built according to the results of the computer simulations. Another reactor of conventional design was also prepared. In order to implement on-line control, a process computer system was used.

CONCLUSIONS AND SIGNIFICANCE

Both the theoretical and experimental aspects of this work have yielded important results. In fact, the balance between theory and practice herein was essential to the success of the investigation. The mathematical model of the dehydrogenation reactor was derived based on fundamental principles and yet was simplified to the extent of being practically useful by a scaling technique which required order-of-magnitude specification of process parameters. This model proved its utility in the design optimization studies since, by its solution, important predictions were made concerning the location of a steam injection port along the reactor and the operating conditions required for optimal reactor performance.

The experimental program complemented the predictions of the model by confirming improved performance by operation of the reactor with a steam injection port. The existence of an optimum of the steam-to-ethylbenzene feed ratio, indicated by simulation using the mathematical model, was demonstrated by experiment.

MATHEMATICAL MODEL

A mathematical model is developed for a styrene pilot plant. In this process, Figure 1, ethylbenzene is passed through a tubular reactor packed with an iron oxide catalyst, and dehydrogenation to styrene takes place. The ethylbenzene feed stream is preheated and mixed with superheated steam to a reactor inlet temperature of over 875°K. More steam may be injected at points along the bed. Since the dehydrogenation reaction is endothermic, there is a temperature drop of as much as 50°K down the reactor, and the residence time is typically 1 s. Superheated steam serves as a diluent, decokes the catalyst extending its life, and supplies sensible heat to keep the reaction temperature up. There are by-product reactions which produce small fractions of benzene and toluene with lighter components, methane and ethylene. The latter

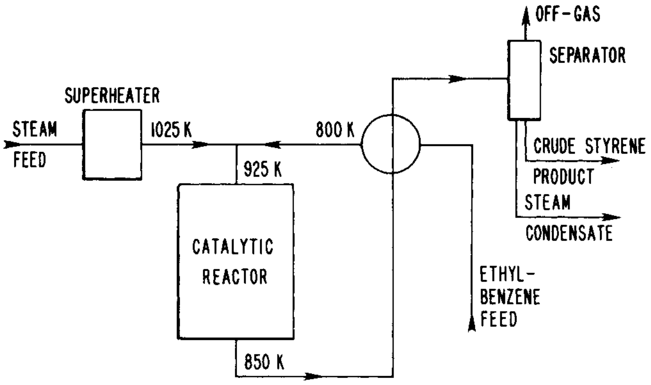

Fig. 1. Adiabatic dehydrogenation process.

Table 1. Significant Chemical Reactions

$C_6H_5CH_2CH_3 \rightleftharpoons C_6H_5CHCH_2 + H_2$
(ethylbenzene) (styrene)
$C_6H_5CH_2CH_3 \rightarrow C_6H_6 + C_2H_4$
(ethylbenzene) (benzene) (ethylene)
$C_6H_5CH_2CH_3 + H_2 \rightarrow C_6H_5CH_3 + CH_4$
(ethylbenzene) (toluene) (methane)
$H_2O + \frac{1}{2} C_2H_4 \rightarrow CO + 2 H_2$
(ethylene)
$H_2O + CH_4 \rightarrow CO + 3 H_2$
(methane)
$H_2O + CO \rightarrow CO_2 + H_2$

Table 2. Rates of Disappearance

j	Species	Reaction rate $- R_j$
1	Ethylbenzene	$R_1' + R_2' + R_3'$
2	Styrene	$- R_1'$
3	Hydrogen	$- R_1' + R_3' - 2R_4' - 3R_5' - R_6'$
4	Benzene	$- R_2'$
5	Toluene	$- R_3'$
6	Methane	$- R_3' + R_5'$
7	Ethylene	$- R_2' + \frac{1}{2} R_4'$
8	Carbon monoxide	$- R_4' - R_5' + R_6'$
9	Carbon dioxide	$- R_6'$
10	Water	$R_4' + R_5' + R_6'$

two can react in water-gas shift reactions to produce more hydrogen, carbon monoxide, then carbon dioxide. A list of the significant chemical reactions appears in Table 1 (Sheel and Crowe, 1969; Wenner and Dybdal, 1948). There are ten distinct chemical species, and the rate of reaction, that is, rate of disappearance, of each species is described in Table 2.

The mathematical model is derived via simplification of the general conservation equations. The reduction of the general equations is made possible by scaling arguments based on reasonable values for system dependent and independent variables. An important approximation which is implied by the model at the outset is that the flow through the packed bed is modeled by mechanical dispersion in both the axial and radial directions.

To develop the thermal energy balance for the fluid phase in the reactor, the fluid is assumed an ideal gas, viscous dissipation effects are neglected, and terms are added for heat sources and sinks due to chemical reaction and internal heat transfer with the catalyst bed. In cylindrical coordinates the result is

$$\rho \overline{c}_v \frac{\partial T}{\partial t} = - \rho \overline{c}_v v \frac{\partial T}{\partial z} + k \frac{\partial^2 T}{\partial z^2} + \frac{\partial k}{\partial z} \frac{\partial T}{\partial z}$$

$$+ \frac{k}{r} \frac{\partial}{\partial r}\left(r \frac{\partial T}{\partial r} \right) + \frac{\partial k}{\partial r} \frac{\partial T}{\partial r} - P \frac{\partial v}{\partial z} + Q_c + Q_r \quad (1)$$

The material balance for species j is

$$\frac{\partial C_j}{\partial t} = - \frac{\partial (v C_j)}{\partial z} + \mathcal{D} \frac{\partial^2 C_j}{\partial z^2} + \frac{\partial \mathcal{D}}{\partial z} \frac{\partial C_j}{\partial z}$$

$$+ \frac{\mathcal{D}}{r} \frac{\partial}{\partial r}\left(r \frac{\partial C_j}{\partial r} \right) + \frac{\partial \mathcal{D}}{\partial r} \frac{\partial C_j}{\partial r} - R_j \quad (2)$$

The equation of motion, simplified by assuming negligible gravitational effects and viscous forces represented by Darcy's law, is

$$\frac{\partial}{\partial t} (\rho v) = - \frac{\partial}{\partial z} (\rho v^2) - \frac{\partial P}{\partial z} - \frac{\mu}{\kappa} v \quad (3)$$

If the component material balance is written for $n - 1$ species, the overall differential material balance, or equation of continuity, for the fluid may be specified without redundancy and is

$$\frac{\partial \rho}{\partial t} = - \frac{\partial}{\partial z} (\rho v) + \frac{w_{si}}{\epsilon A} \delta(z - z_i) \quad (4)$$

The thermal energy balance for the stationary catalyst bed, assuming an effective catalyst bed thermal conductivity k_c and local heat transfer with the fluid, is

$$\rho_c c_{pc} \frac{\partial T_c}{\partial t} = k_c \frac{\partial^2 T_c}{\partial z^2} + \frac{k_c}{r} \frac{\partial}{\partial r}\left(r \frac{\partial T_c}{\partial r} \right) - Q_c \frac{\epsilon}{1 - \epsilon} \quad (5)$$

The heat transfer term is defined as

$$Q_c = \frac{h\hat{A}}{\epsilon} (T_c - T) \quad (6)$$

and the reaction-plus-steam-injection term as

$$Q_r = \sum_j^m R_j' (-\Delta H_j) + \frac{w_{si}}{\epsilon A} h_{si} \delta(z - z_i) \quad (7)$$

These general equations are now simplified by scaling arguments. This scaling method is similar to that described by Krantz (1970) and requires that all variables be made dimensionless by definition of arbitrary scale factors which are chosen such that the dimensionless variables are of order one. Then the differential equations are transformed by substitution of the dimensionless variables with accompanying scale factors. The relative importance of the various terms in the differential equation can be determined by comparison of the various coefficients. When several orders of magnitude difference exist between coefficients, the equation can be justifiably simplified by dropping the small terms.

Some important simplifications of the model due to scaling arguments are presented below. Details are given by Clough (1975).

1. The pressure gradient is negligible in the reactor, and therefore the reactor may be considered to be at constant pressure. In Equation (1), the term $P(\partial v)/(\partial z)$ is negligible, and the heat capacity at constant pressure can be used instead of that at constant volume.

2. Analysis of the mechanisms for heat transport shows the radial dispersion mechanism in the fluid is insignificant when compared to the local catalyst fluid heat transfer, so radial terms in the energy balance [Equation (1)] are dropped. Also, with negligible thermal radial gradients, radial composition gradients can only be generated via boundary condition discontinuities. Since these discontinui-

ties do not exist, radial terms in the material balance [Equation (2)] are judged negligible.

3. Time scaling shows that the axial velocity profile is established very fast compared to temperature and concentration dynamics. Another observation is that the catalyst temperature dynamics are an order-of-magnitude slower than that of the fluid temperature.

4. Axial conduction heat transfer in the catalyst is shown to be negligible; therefore, the axial term in Equation (5) is dropped.

The final set of differential equations describing the reactor system is reduced to

$$\rho \bar{c}_p \frac{\partial T}{\partial t} = - \rho \bar{c}_p v \frac{\partial T}{\partial z} + Q_c + Q_r \tag{8}$$

$$\frac{\partial C_j}{\partial t} = - \frac{\partial (v C_j)}{\partial z} - R_j \tag{9}$$

$$\rho_c c_{pc} \frac{\partial T_c}{\partial t} = \frac{k_c}{r} \frac{\partial}{\partial r}\left(r \frac{\partial T_c}{\partial r} \right) - Q_c \frac{\epsilon}{1 - \epsilon} \tag{10}$$

For any given axial position z, the value of the fluid temperature T in the term Q_c of Equation (10) is constant with respect to radial position r. Then, given the boundary condition that $T_c = T_w$ at the reactor wall, $r = R$, and the symmetry condition that

$$\frac{dT_c}{dr} = 0 \quad \text{at} \quad r = 0 \tag{11}$$

Equation (10) is solved analytically, and the result is

$$T_c(r) - T = (T_w - T) \frac{I_0\left\{ r \sqrt{\dfrac{h\hat{A}}{k_c(1 - \epsilon)}} \right\}}{I_0\left\{ R \sqrt{\dfrac{h\hat{A}}{k_c(1 - \epsilon)}} \right\}} \tag{12}$$

where I_p $(p \geqq 0)$ is the following Bessel function

$$I_p(\bar{\phi}') = \sum_{l=0}^{\infty} \frac{\left(\dfrac{\phi'}{2} \right)^{2l+p}}{l!\,(l+p)!}$$

Equation (12) is substituted into the term for Q_c, and the result is integrated over the radial area from $r = 0$ to $r = R$. This integral is the contribution to thermal energy of the fluid due to convective heat transfer from fluid to catalyst and conductive heat transfer through the catalyst to the wall. To complete the fluid heat transfer term convective heat transfer between fluid and exposed reactor wall is added in, and the result is

$$Q_c = (h_w A_{we} + h \hat{A} \beta_r)(T_w - T) \tag{13}$$

where

$$\beta_r = \frac{2}{\epsilon R \sqrt{\dfrac{h\hat{A}}{k_c(1 - \epsilon)}}} \; \frac{I_1\left\{ R \sqrt{\dfrac{h\hat{A}}{k_c(1 - \epsilon)}} \right\}}{I_0\left\{ R \sqrt{\dfrac{h\hat{A}}{k_c(1 - \epsilon)}} \right\}} \tag{14}$$

Note that all terms in Equation (8) are now invariant with respect to radial position. The model is given by Equations (8), (9), and (13).

It now remains to develop the boundary conditions for Equations (8) and (9) by writing a differential balance for both material and thermal energy at the entrance of the reactor. These are

$$w_f \bar{c}'_{pf} T_f - w_f \bar{c}'_p T + (h_w A_{we} \Delta z + h_w A_{fe})(T_w - T) + \int_\Omega \frac{h\hat{A}}{\epsilon} (T_c - T)\, d\Omega + A \Delta z \sum_j^m R_j' (-\Delta H_j) = 0 \tag{15}$$

and

$$A_t v_f C_{jf} - \epsilon A v C_j - \epsilon R_j A \Delta z = 0 \tag{16}$$

Owing to the mass of metal in the end fitting of the reactor it is assumed that the end catalyst temperature is the same as the wall temperature at $z = 0$. If we take the limit as $\Delta z \rightarrow 0$, we get for the energy balance boundary condition at $z = 0$

$$w_f (\bar{c}'_{pf} T_f - \bar{c}'_p T) + (h\hat{A}\beta_e + h_w A_{fe})(T_w - T) = 0 \tag{17}$$

The effectiveness factor β_e is derived from arguments similar to those used for the radial term and is given by

$$\beta_e = \frac{A}{\sqrt{\dfrac{h\hat{A}}{k_c(1 - \epsilon)}}} \tag{18}$$

For the material balance boundary conditions at $z = 0$

$$\frac{A_t}{\epsilon A} v_f C_{jf} - v C_j = 0 \tag{19}$$

Other auxiliary algebraic relations which are needed to complete the model are:

Concentration of species n (water) is

$$C_n = \frac{P}{R_g T} - \sum_j^{n-1} C_j \tag{20}$$

Fluid density is given by

$$\rho = \sum_j^n C_j M_j \tag{21}$$

Above

M_j = molecular weight of species j

The following gives the linear velocity of the fluid:

$$v = \frac{w_f + \sum_i^p w_{si}\, \delta(z - z_i)}{\rho\, \epsilon\, A} \tag{22}$$

Fluid heat capacity is computed from

$$\bar{c}_p = \frac{\sum_j^n C_j M_j c_{pj}}{\sum_j^n C_j M_j} \tag{23}$$

The spatial derivative of velocity is

$$\frac{\partial v}{\partial z} = - \frac{v}{\rho} \sum_j^n \frac{\partial C_j}{\partial z} M_j \tag{24}$$

and the spatial derivative of C_n is given by

$$\frac{\partial C_n}{\partial z} = -\frac{P}{R_g T^2}\frac{\partial T}{\partial z} - \sum_{j}^{n-1}\frac{\partial C_j}{\partial z} \tag{25}$$

There have been many mathematical models presented for packed-bed catalytic reactors. Froment (1967) compares a one-dimensional, plug flow model (any radial thermal transport lumped at the wall) with a two-dimensional, dispersed flow model. The focus of this work was stability of exothermic reactors. Carberry and White (1969) modeled the oxidation of naphthalene to phthalic anhydride. The goal of their study was to investigate parameter sensitivity via computer simulation. Their model included radial effects in the fluid but ignored catalyst bed conduction.

Hlavacek and Votruba (1974) review most model formulations for adiabatic, packed-bed reactors. Karanth and Hughes (1974) extend a single catalyst particle model to a packed bed for an adiabatic reactor.

The model derived in this work differs from the above in two major aspects:

1. In terms of specific details, end and wall heat transfer effects for both catalyst and fluid have been included here. The effectiveness factor derivations allow for model simplifications. The individual catalyst particle is not modeled here; rather, the volume averaged effect of fluid/catalyst interaction is considered.
2. The simplifications to the complex mathematical model are made on the basis of the scale of the pilot plant reactor used in this work. An attempt has been made to avoid many assumptions which are often used without clear justification.

DESIGN OPTIMIZATION

The mathematical model is now used as a tool in studying, via computer simulation, the operation of the ethylbenzene dehydrogenation reactor. A measure of performance of the reactor system is defined in terms of economic value of reaction products, and this index is used in the optimization of the reactor system. Two strategies are employed in the optimization studies: a simple search method and a gradient projection technique.

Optimization of the reactor system consists of varying operating conditions and design parameters in order to maximize a measure of reactor performance. The first optimization problem is that of a pilot plant reactor for which the steam is entirely mixed with the ethylbenzene stream at the inlet of the reactor. The second configuration allows specification of an injection port part way down the tubular reactor.

Operating conditions which may be varied within constraints are: steam-to-ethylbenzene feed ratio, also commonly steam-to-oil ratio (SOR), expressed on a weight basis; ethylbenzene preheater exit temperature; steam temperature at superheater exit; and the split of steam flow between inlet and reactor injection port, if one is specified. Constraints which are imposed on the above are: steam superheater exit temperature must be less than 1 025°K owing to limitations on materials of construction and electrical heaters, ethylbenzene preheater exit temperature must not exceed 800°K in order to prevent undesirable byproduct reactions in the noncatalytic inlet section before the reactor, the mixture of steam and ethylbenzene streams at the inlet must not exceed 925°K, and the SOR at the reactor inlet must not be less than 1.0 to insure normal catalyst lifetime.

There are certain variables which might have been specified as operating conditions but were not. The feed rate of ethylbenzene will be fixed at an industrially acceptable value, such as a liquid hourly space velocity (LHSV) of 0.75 m^3 ethylbenzene/m^3 catalyst/h. Variation of this rate carries implications to the other steps of the styrene process, especially the refining train downstream. If the reactor optimization can be carried out at an arbitrary LHSV, then it could prove useful as one step in a larger optimization scheme which would vary the ethylbenzene feed rate.

The steam temperature is considered the same at the inlet and any injection port. This is a limitation of the present pilot plant design.

The design parameter which may be varied is the location of an injection port, if one is specified. This is similar to separating the reactor into two vessels in series; however, flexibility is gained in fabrication by using an injection port, and there will be no noncatalytic zone as there is between two reactors in series.

A fourth-order, Runge-Kutta algorithm is used to integrate the steady state form of the material and energy balance equations. With the inlet stream conditions established, the boundary conditions are calculated. The only difficulties in solution center around the nonlinear algebra associated with a variable reactor velocity. In the case that there is a steam injection port along the reactor at some point, a special algorithm is executed which stops the numerical integration, computes a mixing point material and energy balance to account for the steam entering the reactor, and then restarts the integration.

The measure of performance used in the optimization studies has an economic origin; however, it does not reach a level of sophistication whereby capital equipment costs, catalyst depreciation, etc., are included. The performance index is defined by the following formula:

$$PI = C_s F_s - (C_s - C_b) F_b - (C_s - C_t) F_t - C_h F_h \tag{26}$$

where

C_s : styrene value, \$44.20/kgmole

C_b : benzene value, \$21.13/kgmole

C_t : toluene value, \$17.65/kgmole

C_h : steam cost, \$$(0.0079 + 4.29 \times 10^{-5} T(°K))$/kgmole

F_s, F_b, F_t, F_h : flow rates of styrene, benzene, toluene and steam in kgmole/day

The styrene, benzene, and toluene values are commodity prices from November, 1974. The formula used for cost of steam is that of Sheel and Crowe (1969) except that it has been inflated to reflect increase in energy cost over the years since their work. The value of other by-products, such as fuel value of the off-gas, is not treated. These factors are small compared to those of the performance index above and will not shift the optimum significantly. This is not to say, though, that the fuel value of the off-gas should be ignored in the overall operation of a plant. In order to give easily handled numbers, grams produced in the pilot plant are interpreted as kilograms in the performance index.

The first strategy used in the optimization studies was a simple search over reasonable ranges of the operating conditions and port position, if any. Although this method is inefficient and unsophisticated, it does provide a good feel for the nature of the performance surface. For example, that the optimum lies on a constraint is readily determined by search, and such a conclusion can greatly simplify the optimization problem.

The second strategy employed was a gradient projection technique due to Rosen (1960). The experience with this technique was that it wasted much time testing constraints which, by the search method, were already known to be active at the optimum.

OPTIMIZATION RESULTS

The first problem is that of the reactor with no steam injection port. The results of the optimization are best depicted as a map of the optimization surface as shown in Figure 2. The kinetic expressions used to obtain these results are given in Table 3, where the numerical values given are those of Sheel and Crowe (1969). The constraint on preheater exit temperature is always active and so is not shown on the figure. For a liquid hourly space velocity (LHSV) of ethylbenzene equal to 0.75, the optimum lies on the constraint of maximum inlet temperature, and the operating conditions are:

1.	Steam-to-oil ratio	1.6
2.	Steam temperature at superheater exit	1 019°K
3.	Ethylbenzene temperature at preheater exit (constraint active)	800°K

The value of the performance index at this point is \$71.83/day. Temperature, conversion of ethylbenzene, and selectivity to styrene as functions of reactor position are presented in Figure 3 for this case.

Since the performance of the simulated reactor is highly dependent on the rate of reaction of ethylbenzene to styrene, uncertainty in estimation of the kinetic parameters of this reaction, the frequency factor, and activation energy could lead to erroneous results in the selection of the optimal operating point. For this reason, the first optimization problem was solved for reasonable variations of the kinetic parameters. The results of this study are presented in Figure 4 as a steam-to-oil ratio surface for different values of frequency factor and activation energy. Note the high sensitivity of the optimal SOR to variations in these parameters.

The second optimization problem adds to the first a design variable, the location of the injection port, and an additional operating variable, the split of steam between the inlet and injection ports. The first step taken to study this problem was to determine if an improvement could be made by splitting the optimal value of steam flow of the first problem in two equal parts and allowing the injection port location to vary. The results of this investigation are presented in Figure 5. An improvement in performance index of more than 4% is noted, with the injection port located approximately 20% of the length of the reactor as measured from the entrance. Figure 5 also shows that, at that fixed port location, variation in steam distribution from a 50-50 split to 37.5% in the inlet yields an additional marginal improvement.

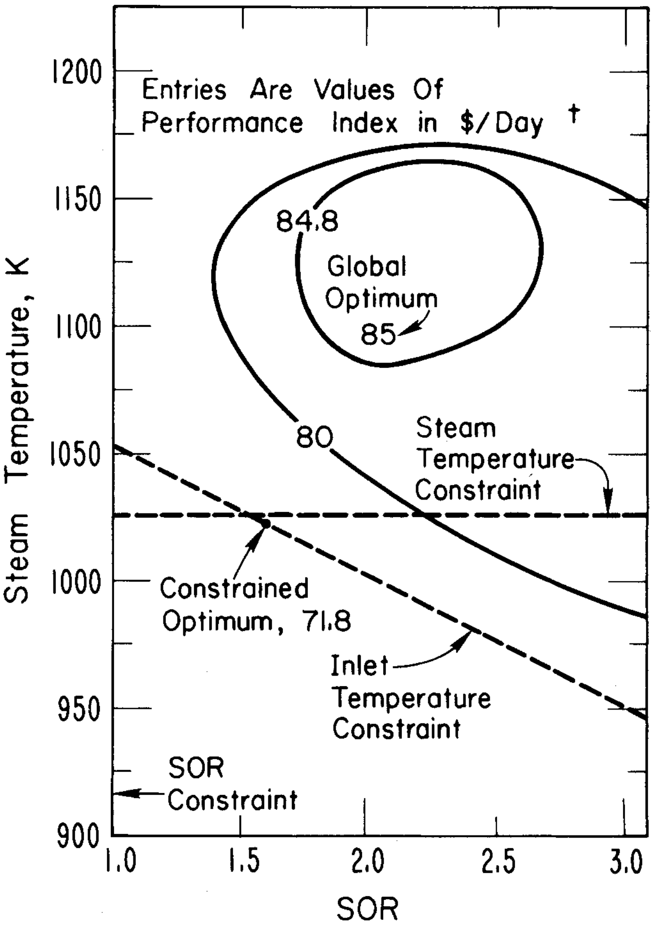

† Basis = 0.75 LHSV = 480 kg EB Feed/Day

Fig. 2. Optimal reactor conditions.

TABLE 3. REACTION KINETICS

Ethylbenzene dehydrogenation

$$R_1' = k_1(C_1 - C_2C_3/K_e)$$

$$k_1 = \frac{R_gT\omega_e}{P_a}\exp(F_1 - E_1/R_gT)$$

$$K_e = \frac{P_a}{R_gT}\exp(16.12 - 15\,350/T)$$

Dealkylation to benzene

$$R_2' = k_2C_1 \qquad k_2 = \frac{R_gT\omega_e}{P_a}\exp(13.24 - 49\,675/R_gT)$$

Dealkylation to toluene

$$R_3' = k_3C_1C_3 \qquad k_3 = \left(\frac{R_gT}{P_a}\right)^2 \omega_e \exp(0.2961 - 21\,857/R_gT)$$

Water-ethylene shift

$$R_4' = k_4C_{10}\sqrt{C_1} \qquad k_4 = \left(\frac{R_gT}{P_a}\right)^{3/2} \omega_e \exp(-0.0724 - 24\,838/R_gT)$$

Water-methane shift

$$R_5' = k_5C_6C_{10} \qquad k_5 = \left(\frac{R_gT}{P_a}\right)^2 \omega_e \exp(-2.934 - 15\,697/R_gT)$$

Water-carbon monoxide shift

$$R_6' = k_6C_8C_{10}\frac{P}{R_gT} \qquad k_6 = \left(\frac{R_g}{P_a}\right)^3 \omega_e \exp(21.24 - 17\,585/R_gT)$$

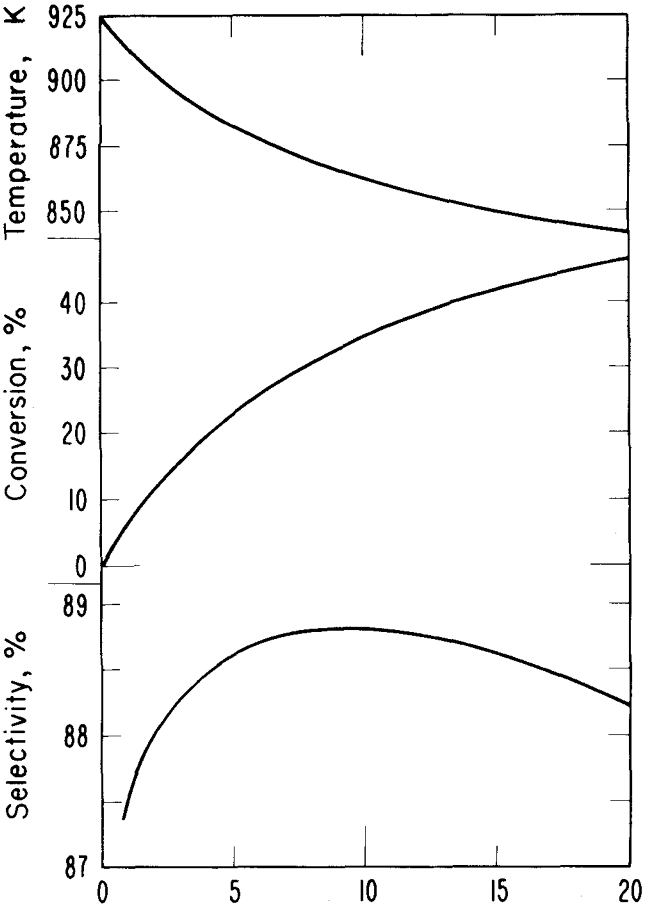

Fig. 3. Reactor profiles.

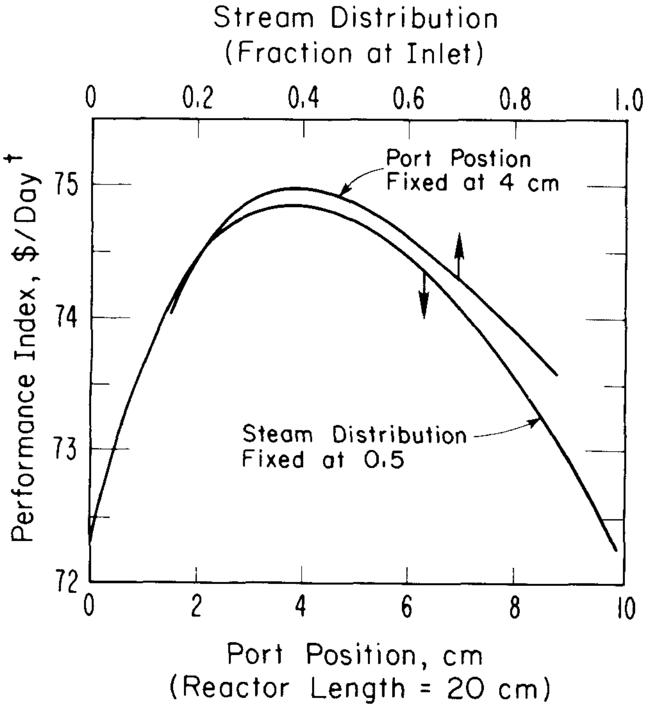

† Basis = 0.75 LHSV = 480 kg EB Feed/Day

Fig. 5. Optimization of injection port.

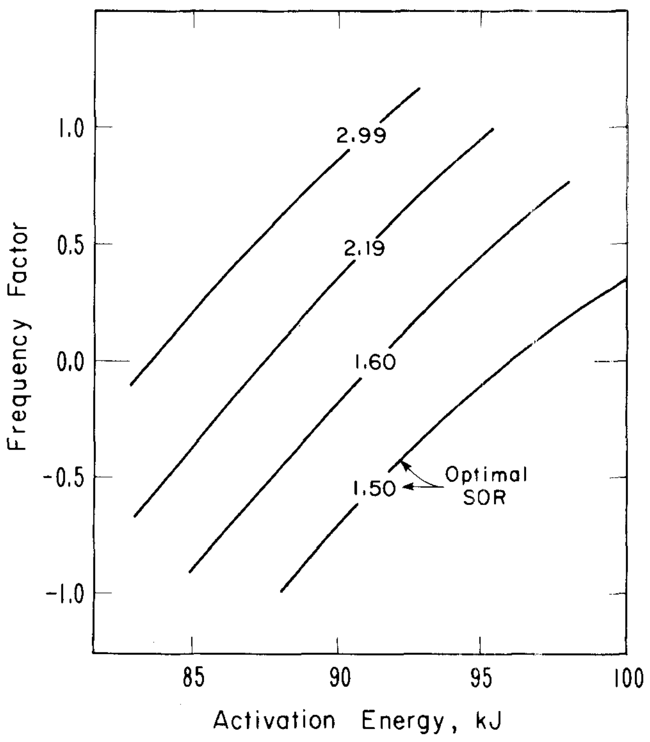

Fig. 4. SOR vs. kinetic parameters.

The restriction to the same amount of steam as for the first problem's optimum is now lifted. Optimization with the variables of port location, steam-to-oil ratio, steam distribution, steam temperature, and ethylbenzene temperature at preheater exit (always at constraint) has been carried out by both search and gradient techniques to yield similar results:

1. Port location at 28.6% of length of reactor from inlet.
2. Steam-to-oil ratio of 2.76.
3. Steam distribution of 37.8% to inlet port, remainder to injection port.
4. Steam temperature at the constraint of 1 025°K.
5. Ethylbenzene temperature at preheater exit also at its constraint value of 800°K.

The performance index for the above conditions is \$81.10/day, a gain over the optimum of the first problem of nearly 13%.

There appears to be much to gain in designing a reactor with at least one steam injection port. The optimum for this problem is more sensitive to port location and steam-to-oil ratio than to steam distribution. Sensitivity to steam temperature would be high if that temperature were unconstrained.

STYRENE PILOT PLANT

A diagram of the pilot plant is provided as Figure 6. The dehydrogenation reactor is constructed of a 7-in. (177.8 mm) section of pipe [1 in. (25.4 mm) nominal diameter, schedule 40, stainless steel type 316] with 1 in. (25.4 mm) lengths of small seamless tube [⅛ in. (6.35 mm) outside diameter, stainless steel type 316] welded into the wall of the pipe to give access for installing thermocouples and for an injection port. The reactor pipe has 1 in. (25.4 mm) pipe threads at both ends. A cap is screwed on to each end to complete the reactor unit. The caps were machined out of 2 in. (50.8 mm) diameter, stainless steel type 316 barstock, and a 1 in. (25.4 mm) length of seamless tubing [¼ in. (6.35 mm) outside diameter] is welded into each cap to allow access to the reactor for inlet and exit streams. When assembled, the

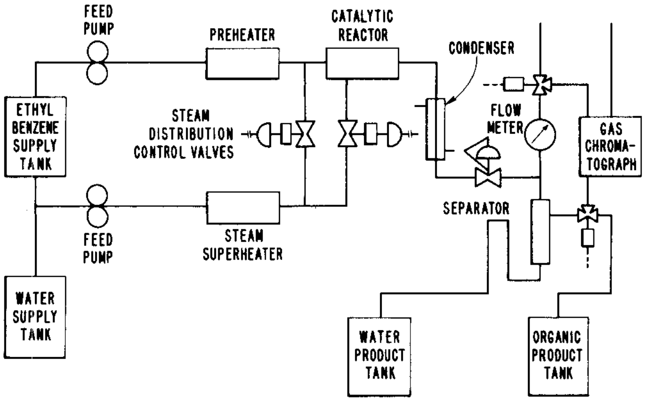

Fig. 6. Styrene pilot plant.

reactor is packed with cylindrical pellets [1/8 in. (3.18 mm) diameter] of Shell 105 catalyst. A few small berl saddles are also packed into the reactor at each end to prevent the catalyst from slipping out of the reactor via the exit and entry tubes.

The steam superheater and ethylbenzene preheater vessels are of similar construction to that of the reactor except that only one thermocouple port is installed midway along the pipe and the packing is totally of berl saddles. Connecting links between reactor and other vessels are all of seamless, stainless steel type 316 tube [1/4 in. (6.35 mm) outside diameter] secured by ferrule types of tube fittings.

Water and ethylbenzene are supplied from two stainless steel tanks which may be pressurized by air. The two feed pumps shown on Figure 6 are actually the two sides of a duplex Milton Roy Instrument miniPump®, a precision, positive-displacement metering pump with operable range of 16 to 400 cm^3/h of liquid. The pump feed lines are filtered, and the discharge lines are equipped with back pressure regulators [100 lb/in.^{2} gauge (690 kPa)] and pressure gauges. The valves used for control of superheater pressure and steam distribution are miniature, pneumatic Research control valves supplied by Precision Products Division of Badger Meter Company (trim size N, maximum $C_v = 0.006$, trim material solid Stellite, finned bellows) with integral, top mounted Moore positioners.

After the reactor exit, there is a simple condenser which consists of a 1 in. carbon steep pipe jacketing the 1/4 in. stainless steel exit tube. Cold tap water is piped into the steel pipe jacket. Although pressure in the steam superheater is regulated by the distribution valves, pressure in the reactor and preheater is controlled by a Fisher Controls back pressure regulator downstream of the condenser set at 5 lb/in.^{2} gauge (34.5 kPa).

After the reactor pressure regulator, there is a series of elements of the pilot plant whose function is to separate and analyze the product stream. Noncondensable products, such as hydrogen, separate from the liquid products and travel upward through a sealed drum, wet test gas meter, through the sample loop of an automatic gas sample valve (Microtek), and to the vent. Liquid products, water, and organic phases are separated by gravity in a 100 cm^3, vertical, cylindrical glass vessel. The water phase goes underneath and is collected in a product vessel, and the organic product comes over the top in the separator and passes through an automatic liquid sample valve (Tracor) after which it drops into another product vessel.

Analysis of the off-gas and liquid streams is made possible by the combination of the above-mentioned automatic sample valves and a modified Beckman GC-5 gas chromatograph. One of the dual columns of the chromatograph serves to analyze the liquid stream, while the other is used as the carrier gas reference column. Alternately, the off-gas stream is sampled into the latter column, and the liquid column serves as the reference for gas analysis. The liquid analysis column is a coil made from a 2 m long, 1/4 in. tube of stainless steel type 316. The column packing is a solid support of Chromosorb W (60 to 80 mesh) treated with a liquid phase of diisodecylphthalate which is 15% of the weight of the solid support (Spencer, 1963). The column for analysis of the off-gas is also of 1/4 in. (6.35 mm) stainless steel tubing; however, it is 2.5 m long and packed with Porapak Type Q-S (80 to 100 mesh).

The preheater and superheater vessels are each wrapped with 1 500 W, beaded, nichrome wire heaters (Marsh). The tubes from the superheater to distribution valves and on to reactor are traced with lower wattage beaded heaters. Also, the reactor is wrapped with two beaded heaters. Each of the electrical heaters is connected to a solid state relay which may be controlled by an external 5 V signal. All heated parts of the pilot plant are wrapped with 4 to 6 in. (about 125 mm) thickness of Fiberfrax insulation (Carborundum).

In order to insure safe operation and to provide sufficient measurement information and capability for control, the pilot plant has been instrumented heavily. Safety relief valves are installed upstream of the superheater and preheater as are overpressure switches which can cut power to the respective 1 500 Watt heaters. Thermocouples installed in both preheater and superheater berl saddle beds are connected to overtemperature switches which also will turn off the heaters if a high temperature condition exists.

Upstream of the steam superheater there is a strain gauge pressure transducer (Dynisco) installed to measure the superheater pressure. A bridge transmitter unit provides a voltage signal proportional to pressure. Numerous additional thermocouples, all type K, chromel-alumel, protected by 1/16 in. (1.6 mm) stainless steel sheaths, are installed in the pilot plant. All of these thermocouples lead via twisted, shielded extension wire to a junction box where a cable changeover is made to normal signal transmission wire. The temperature of the junction box is measured with a platinum resistance thermometer connected to a bridge transmitter which has a convenient voltage output.

The stroke of the metering pumps is usually adjusted manually by turning two micrometer style dials. The pilot plant unit was modified. Two dual shafted stepping motors were mounted on the dial shafts and the control instruments fabricated so that the pumps' strokes can be controlled externally. Multiturn potentiometers were coupled to the opposite motor shafts to provide a position measurement for feedback control.

The off-gas flow rate for such a small pilot plant is less than 5 cm^3/s; therefore, measurement over a short interval is difficult. A high resolution digital optical encoder (4 800 pulses/revolution) was coupled to the shaft of the wet test meter so that its slow rotation could be measured.

The sampling valves of the gas chromatograph have been equipped with cylinder operators which are driven using compressed air and four-way solenoid valves. The steam distribution control valves are driven by air pressure from Fisher current-to-pneumatic converters.

DATA ACQUISITION AND CONTROL COMPUTER SYSTEM

A process computer system was designed and fabricated for use in automation of the styrene pilot plant. This system is based on a Data General Nova 1210 minicomputer with 24K words of magnetic core memory. The process interface includes thirty-two analogue inputs, four analogue outputs, sixteen digital inputs, and sixteen digital outputs. Analogue input signals from the pilot plant in-

TABLE 4. STEAM-TO-OIL RATIO (SOR) OPTIMIZATION

Condition	SOR	Conversion	Selectivity	Performance
1	1.36	74.1 ± 1.0	87.9 ± 0.6	120.5
2	1.46	76.0 ± 0.7	89.3 ± 0.5	127.9
3	1.70	76.7 ± 0.7	90.9 ± 0.4	132.0
4	2.06	80.7 ± 1.2	90.0 ± 1.0	137.2
5	2.48	82.3 ± 0.6	86.9 ± 1.6	131.1

cluded seventeen thermocouples and other measurements such as steam pressure and chromatograph thermal conductivity cell output. Two analogue outputs were used to drive the control valves. Digital input signals were those of the wet test meter's optical encoder and the temperature and pressure switches. Seven of the digital outputs were employed to control the electrical heaters via solid state relays, and others were used to control the feed pumps.

An extension of BASIC, a high-level interpreter computer language, was used as the programming system for the monitoring and control of the styrene pilot plant. The modifications to the BASIC interpreter required for communication with the process in real time were implementation of a CALL function which allows special subroutines necessary for handling of peripheral devices, and extension of the interpreter's interrupt-handling routine which initially only serves the teletype unit. Eighteen CALL subroutines were implemented for use with the pilot plant.

By use of a high-level, multiple-task programming scheme, many independent program segments were implemented to acquire data and control the pilot plant. Details of the computer program have been documented elsewhere (Clough, 1975).

EXPERIMENTAL PROGRAM

Two specific experimental investigations were carried out. Simulation studies showed that for the conventional dehydrogenation reactor with no steam injection port, an optimal steam-to-ethylbenzene feed ratio (SOR) is found on either the constraint temperature of the reactor inlet or of the exit of the steam superheater depending on process conditions. In fact, this optimal SOR value was shown to be sensitive to variations in the kinetic parameters of the main dehydrogenation reaction. The first experimental investigation was then to search out and confirm the existence of an optimum in SOR. The computer simulations also indicated that by splitting the steam between the inlet and an appropriately located injection port along the reactor, a marked improvement in process performance should be noted even at the same overall SOR established without the injection port. It was desirable to test the validity of this prediction by experiment.

A series of experimental conditions were achieved, each with a different water pumping rate, or SOR. At each condition, at least four and as many as six chromatograph analyses formed the data base for computing the performance of the reactor. As each new SOR value was established, the electrical heaters were controlled to maintain the same inlet temperature (913°K). The initial SOR value was low, 1.36; for subsequent conditions, the value was increased as long as the performance also improved. The results of this evolutionary procedure are reported in Table 4. As the water rate was increased, the conversion steadily rose; however, the selectivity to styrene passed through a maximum as did the performance measure. The optimal SOR appears to be in the neighborhood of two. After temperature data were studied which were acquired during the time when the above conditions were established, it was concluded that the zone heaters on the reactor were running at a duty cycle sufficiently high to provide sensible heat to the reactor rather than remain approximately adiabatic. Therefore, given true adiabatic conditions, the optimal SOR would be higher than the value determined, since some of the thermal energy formerly provided by the heaters would be provided by steam. Estimation of kinetic parameters was carried out during the experiment based on measurements of temperature along the reactor and composition of the effluent. A sequential filter technique (Clough and Ramirez, 1976) yielded the values for the parameters of the dehydrogenation reaction:

$$\text{activation energy } (E_1) = 77.5 \text{ kJ}$$

$$\text{frequency factor } (F_1) = -1.0$$

By extrapolation of Figure 4, the optimum SOR value for the above parameters will fall in the band between the contours of 2.19 and 2.99.

The kinetic parameters determined by Sheel and Crowe (1969) were

$$\text{activation energy } (E_1) = 90.0 \text{ kJ}$$

$$\text{frequency factor } (F_1) = -0.0854$$

and these values yield an optimum SOR of 1.6 by our calculations as shown in Figure 4.

Following the evolutionary optimization, the condition of SOR approximately equal to two was reestablished, except now with lower duties on the reactor zone heaters. As a result the performance was reduced owing to less conversion. Without changing the overall steam rate, the injection control valve was opened, and the loading on the two valves was set by the computer at the simulated optimal ratio of 0.375 inlet/injection. The electrical heaters at the inlet and injection port were readjusted to give the required temperatures for direct comparison with the no-injection case. Steam pressure was controlled via the computer by adjusting both inlet and injection valves in unison. The change in reactor performance from the inlet only to the injection case is noted in Table 5. An improvement of more than 9% is evident. Therefore, it has been demonstrated that there is a significant benefit in dividing the steam flow between the reactor inlet and one injection port.

TABLE 5. IMPROVEMENT DUE TO STEAM INJECTION

SOR	Conversion	Selectivity	Performance
Inlet only case			
2.04	72.4 ± 0.3	90.0 ± 0.7	122.6
Injection case			
2.04	85.8 ± 0.9	85.2 ± 1.3	134.1

Nine percent improvement in injection case.

CONCLUSIONS

Both the theoretical and experimental aspects of this work have yielded results of importance. In fact, the balance between theory and practice herein was essential to the success of the investigation. The mathematical model of the dehydrogenation reactor was derived based on fundamental principles yet was simplified to the extent of being practically useful by a scaling technique which required specification of process parameters. This model proved its utility in the design optimization studies since, by its solution, important predictions were made concerning the location of a steam injection port along the reactor and the operating conditions required for optimal reactor performance.

The experimental program complemented the predictions of the model by confirming improved performance by operation of the reactor with a steam injection port. The existence of an optimum of the steam-to-ethylbenzene feed ratio, indicated by simulation using the mathematical model, was demonstrated by experiment.

ACKNOWLEDGMENT

The authors wish to acknowledge financial support from the National Science Foundation (grants GK35861 and GK34234) for this work. Valuable technical advice was also provided by the Dow Chemical Company—Texas Division. Shell Chemical Company provided catalyst for the work, and Badger Meter Company allowed a generous discount in the purchase of their control valves.

NOTATION

A = cross-sectional area of reactor tube
$\hat{A}$ = area of catalyst pellet surface per volume of packed bed
A_{fe} = area of end flange exposed to fluid
A_t = cross-sectional area of feed tube
A_{we} = area of wall exposed to fluid per length
C_b = benzene value
C_h = steam cost
C_j = concentration of species j
C_s = styrene value
C_t = toluene value
$\bar{c}_p$ = weighted average of heat capacities at constant pressure
$\bar{c}_p'$ = mean heat capacity of fluid from 0°C to temperature T at constant pressure
c_{pc} = heat capacity at constant pressure of catalyst
c_{pj} = heat capacity at constant pressure of species j
$\bar{c}'_{pf}$ = mean heat capacity of fluid in feed tube from 0°C to temperature T at constant pressure
$\bar{c}_v$ = weighted average of heat capacities at constant volume
$\mathcal{D}$ = mass dispersion coefficient
F_b = molar flow rate of benzene
F_h = molar flow rate of steam
F_s = molar flow rate of styrene
F_t = molar flow rate of toluene
h_{si} = specific enthalpy of steam in port i
h_w = heat transfer coefficient between fluid and wall
$I_p(\cdot)$ = Bessel function
j = index
k = dispersion analogue of thermal conductivity
k_c = effective thermal conductivity of catalyst bed
k_i = $i = 1$ to 6, reaction rate parameter group
k_e = equilibrium constant for main reaction
l = index
m = index, or number of reactions, 6
M_j = molecular weight of species j
p = number of steam ports
P = total pressure
P_a = ambient pressure
Q_c = heat transfer between fluid and catalyst, rate per volume of bed
Q_r = heat source/sink due to reaction and injection
r = radial spatial independent variable
R = inside radius of reactor tube
R_g = gas law constant, units as appropriate
R_j = rate of disappearance of species j
R_j' = rate of reaction j
t = time
T = temperature of fluid
T_c = temperature of catalyst
T_f = temperature of reactor feed
T_w = temperature of wall
v = average linear axial velocity of fluid in reactor
w_f = mass flow rate in feed
w_{si} = mass flow rate of steam in port i
z = axial spatial independent variable
z_i = location of injection port i

Greek Letters

β_e = end effectiveness factor
β_r = radial effectiveness factor
$\delta(\cdot)$ = Dirac measure
Δz = axial dimension of differential element
ΔH_j = heat of reaction j
ϵ = porosity of packed bed
κ = permeability of packed bed
μ = fluid viscosity
Ω = volume element
ρ = mass density
ρ_c = mass density of catalyst pellet
ω_e = catalyst weight per reactor void volume

LITERATURE CITED

Carberry, J. J., and D. White, "On the Role of Transport Phenomena in Catalytic Reactor Behavior," *Ind. Eng. Chem.*, **16**, 27-35 (July, 1969).

Clough, D. E., "Optimization and Control of the Dehydrogenation of Ethylbenzene to Form Styrene," Ph.D. dissertation, Univ. Colo., Boulder (1975).

———, and W. F. Ramirez, "On-line Estimation and Identification of a Nonlinear, Distributed-parameter Process: The Dehydrogenation of Ethylbenzene to Form Styrene in a Tubular, Fixed-bed, Catalytic Reactor," under review for publication in *Chem. Eng. Sci.* (1976).

Froment, G. F., "Fixed-bed Catalytic Reactors," *Ind. Eng. Chem.*, **59**, 18-27 (Feb., 1967).

Hlavacek, V., and J. Votruba, "Experimental Study of Multiple Steady States in Adiabatic Catalytic Systems," in *Chemical Reaction Engineering III, Advances in Chemistry Series #133*, H. M. Hulburt, ed., p. 545, American Chemical Society (1974).

Karanth, N. G., and R. Hughes, "Temperature and Concentration Gradients in a Catalytic Packed-bed Reactor," *Chemical Reaction Engineering III, Advances in Chemistry Series #133*, H. M. Hulburt, ed., p. 449, American Chemical Society (1974).

Krantz, W. B., "Scaling Initial and Boundary Value Problems *Chem. Eng. Educ.* (Summer, 1970).

Rosen, J. B., "The Gradient Projection Method of Nonlinear Programming, "Part I: Linear Constraints," *SIAM*, **8**, 1 (March, 1960); "Part II: Nonlinear Constraints," 9, 4 (Dec., 1961).

Sheel, J. C. P., and C. M. Crowe, "Simulation and Optimization of an Existing Ethylbenzene Dehydrogenation Reactor," *Can. J. Chem. Eng.*, **47**, 183 (1969).

Spencer, S. F., "Rapid Separation of Xylenes and Ethylbenzene by Gas Chromatography Using Packed Columns," *Anal. Chem.*, **35**, 592 (1963).

Wenner, R. R., and E. C. Dybdal, "Catalytic Dehydrogenation of Ethylbenzene," *Chem. Eng. Progr*, **44**, No. 4, 275 (Apr., 1948).

Manuscript received June 28, 1976; revision received September 15 and accepted September 16, 1976.